Inhibition of phosphoglucomutase activity by lithium alters cellular calcium homeostasis and signaling in Saccharomyces cerevisiae

Péter Csutora, András Strassz, Ferenc Boldizsár, Péter Németh, Katalin Sipos, David P. Aiello, David M. Bedwell and Attila Miseta

Am J Physiol Cell Physiol 289:58-67, 2005. First published Feb 9, 2005; doi:10.1152/ajpcell.00464.2004

Am J Physiol Cell Physiol 289: C58–C67, 2005.
First published February 9, 2005; doi:10.1152/ajpcell.00464.2004.

Inhibition of phosphoglucomutase activity by lithium alters cellular calcium homeostasis and signaling in *Saccharomyces cerevisiae*

Péter Csutora,[1] András Strassz,[1] Ferenc Boldizsár,[2] Péter Németh,[2] Katalin Sipos,[3] David P. Aiello,[4] David M. Bedwell,[4] and Attila Miseta[1]

[1]*Department of Laboratory Medicine,* [2]*Department of Immunology and Biotechnology, and* [3]*Department of Biochemistry, Faculty of Medicine, Pécs University, Pécs, Hungary; and* [4]*Department of Microbiology, University of Alabama at Birmingham, Birmingham, Alabama*

Submitted 21 September 2004; accepted in final form 8 February 2005

Csutora, Péter, András Strassz, Ferenc Boldizsár, Péter Németh, Katalin Sipos, David P. Aiello, David M. Bedwell, and Attila Miseta. Inhibition of phosphoglucomutase activity by lithium alters cellular calcium homeostasis and signaling in *Saccharomyces cerevisiae*. *Am J Physiol Cell Physiol* 289: C58–C67, 2005. First published February 9, 2005; doi:10.1152/ajpcell.00464.2004.—Phosphoglucomutase is a key enzyme of glucose metabolism that interconverts glucose-1-phosphate and glucose-6-phosphate. Loss of the major isoform of phosphoglucomutase in *Saccharomyces cerevisiae* results in a significant increase in the cellular glucose-1-phosphate-to-glucose-6-phosphate ratio when cells are grown in medium containing galactose as carbon source. This imbalance in glucose metabolites was recently shown to also cause a six- to ninefold increase in cellular Ca^{2+} accumulation. We found that Li^+ inhibition of phosphoglucomutase causes a similar elevation of total cellular Ca^{2+} and an increase in $^{45}Ca^{2+}$ uptake in a wild-type yeast strain grown in medium containing galactose, but not glucose, as sole carbon source. Li^+ treatment also reduced the transient elevation of cytosolic Ca^{2+} response that is triggered by exposure to external $CaCl_2$ or by the addition of galactose to yeast cells starved of a carbon source. Finally, we found that the Ca^{2+} overaccumulation induced by Li^+ exposure was significantly reduced in a strain lacking the vacuolar Ca^{2+}-ATPase Pmc1p. These observations suggest that Li^+ inhibition of phosphoglucomutase results in an increased glucose-1-phosphate-to-glucose-6-phosphate ratio, which results in an accelerated rate of vacuolar Ca^{2+} uptake via the Ca^{2+}-ATPase Pmc1p.

calcium influx; calcium signal; galactose; glucose phosphate

LITHIUM IS COMMONLY USED CLINICALLY either alone or in combination with valproic acid or carbamazepine for the treatment of bipolar disorder (11, 31). Also, it is the oldest mood stabilizer that remains in clinical use (38). Despite extensive research, the exact molecular mechanism(s) of Li^+ action remain(s) unknown (24, 37). Two molecular targets for Li^+ at therapeutically relevant concentrations (0.6–1.2 mmol/l serum) are inositol monophosphatase and glycogen synthase kinase (GSK)-3β, both important enzymes of intracellular signal transduction pathways (7, 17). The third molecular target of Li^+, phosphoglucomutase (PGM) (18, 37), is a key metabolic enzyme of reserve polysaccharide synthesis and galactose (Gal) metabolism (14, 25).

The effect of Li^+ on inositol metabolism was described during the 1970s (4), and a relationship between altered inositol metabolism and cellular Ca^{2+} signaling was elucidated during the early 1980s (8). Briefly, Li^+ inhibits inositol monophosphatase. Therefore, Li^+ therapy results in the accumulation of inositol monophosphate and a decrease of free inositol in the brain, which is thought to result in decreased neuronal Ca^{2+} mobilization (1). Alternative proposals to explain how Li^+ modifies cellular signaling have suggested that it decreases protein kinase C activity, G protein activation, or cAMP generation (1, 16, 43). It has also been reported that Li^+ inhibits GSK-3β activity (23, 40). Some developmental, metabolic, and neuroprotective actions of Li^+ could be readily explained by a negative regulation of GSK-3β function (18, 23, 40). Li^+ inhibits the activity of these proteins (and other enzymes not directly involved in signal transduction) by competitively displacing Mg^{2+} from its binding site (35, 36). Enzymes such as inositol phosphatases, fructose 1,6-bisphosphatase, and bisphosphate nucleotidases all share a structural domain for Mg^{2+} binding (44). The Mg^{2+} binding domain of PGM is different, but Li^+ also competitively displaces Mg^{2+} from its binding site on PGM, thus reducing its enzymatic activity (26, 36).

PGM catalyzes the reversible conversion of glucose (Glc)-1-phosphate (Glc-1-P) to Glc-6-phosphate (Glc-6-P). This function leads to its involvement in the synthesis and degradation of UDP-hexoses and glycogen, as well as in Gal metabolism. The direction of metabolic flow through PGM depends on the carbon source available (Fig. 1). *Saccharomyces cerevisiae* has two PGM genes, *PGM1* and *PGM2*, with the latter accounting for ~80–90% of the total activity (14). At least one of the *PGM* genes is required for cell growth in media containing Gal, but not Glc, as sole carbon source. Recently, we reported (15) that a *pgm2*Δ strain lacking the major isoform of PGM accumulates six- to ninefold more total cellular Ca^{2+} (Ca_t) than a wild-type strain. Furthermore, this Ca^{2+} overaccumulation occurred in Gal-containing media, in which the intracellular Glc-1-P level is severalfold higher than normal, but not in media containing Glc as carbon source. The increase in Ca_t observed in cells grown with Gal as carbon source is due to an elevated rate of Ca^{2+} influx across the plasma membrane (15). We found (2) that the altered Ca^{2+} homeostasis phenotypes (including high Ca_t and increased Ca^{2+} uptake through the plasma membrane) in the *pgm2*Δ strain are suppressed in a mutant *S. cerevisiae* strain that lacks the regulatory subunit of phosphofructokinase (PFK2). This *pgm2*Δ/*pfk*Δ strain contained elevated levels of both Glc-1-P and Glc-6-P when grown in media containing Gal as carbon source. This finding led to

Address for reprint requests and other correspondence: A. Miseta, Pécs Univ., Faculty of Medicine, Dept. of Laboratory Medicine, Ifjúság u. 13, 7624 Pécs, Hungary (e-mail: attila.miseta@aok.pte.hu).

The costs of publication of this article were defrayed in part by the payment of page charges. The article must therefore be hereby marked "*advertisement*" in accordance with 18 U.S.C. Section 1734 solely to indicate this fact.

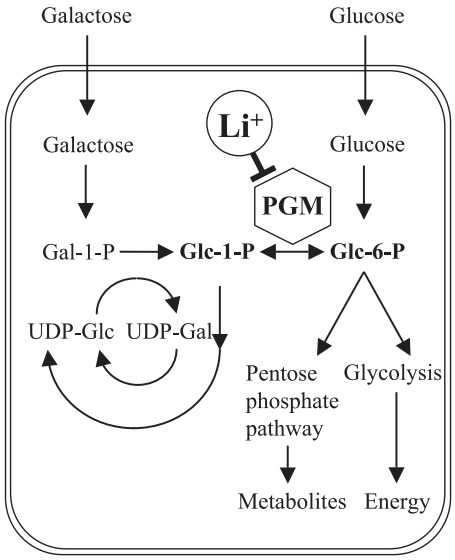

Fig. 1. Major metabolic pathways that require phosphoglucomutase (PGM) activity in eukaryotic cells. Note that PGM activity is essential when galactose (Gal) is utilized as the sole carbon and energy source. Glc, glucose; Gal-1-P, galactose-1-phosphate; Glc-1-P, glucose-1-phosphate; Glc-6-P, glucose-6-phosphate.

the conclusion that cellular Ca^{2+} homeostasis is linked to the intracellular Glc-1-P-to-Glc-6-P ratio, and thus to PGM activity, in *S. cerevisiae*. Recently, we reported (3) that the disruption of the *PMC1* gene encoding the vacuolar Ca^{2+}-ATPase Pmc1p also suppressed the Ca^{2+}-related phenotypes in the *pgm2*Δ strain, suggesting an important role for vacuolar Ca^{2+} compartmentalization. We also noted that the grossly increased unfolded protein response in the *pgm2*Δ mutant is probably a consequence of unbalanced (predominantly vacuolar) Ca^{2+} storage, which results in a reduced endoplasmic reticulum (ER) Ca^{2+} level.

These observations prompted us to investigate whether the inhibition of PGM activity by Li^+ could influence cellular Ca^{2+} homeostasis and signaling in *S. cerevisiae*. Our results indicate that exposure to Li^+ induces excessive Ca^{2+} uptake and accumulation in a manner that is extremely similar to the phenotype previously observed in the *pgm2*Δ mutant. Because these perturbations in Ca^{2+} homeostasis can be suppressed by disruption of the gene encoding the vacuolar Ca^{2+}-ATPase Pmc1p (*pmc1*Δ), we conclude that they result from hyperactivation of the vacuolar Ca^{2+}-ATPase Pmc1p.

MATERIALS AND METHODS

Cell lines and culture conditions. S. cerevisiae strains used in the present study include SC252 (Sj21R) (*MATa ade1 leu2, 3–112 ura3–52 MEL*), YDB200 (*MATa ade1 leu2,3–112 ura3–52 pgm1*Δ*::URA3*) and YDB171 (*MATa ade1 leu2, 3–112 ura3–52 pgm2*Δ*::LEU2, MEL*). *S. cerevisiae* strains were grown in standard yeast extract-peptone (YP) medium or synthetic minimal (SM) medium supplemented with either 2% D-Glc or 2% D-Gal as carbon source. In all experiments, cultures were grown for at least 5–6 generations to a cell density of ≤1.0 absorbance at 600 nm (A_{600}) unit/ml.

Measurement of Ca_t levels, Ca^{2+} uptake rates, and Ca^{2+} exchange. Ca_t levels were measured with an Eppendorf Efox 5053 flame photometer (27, 28). Briefly, cells were grown to a cell density of 0.8–1.0 A_{600} units/ml and then harvested by centrifugation at room temperature (RT) for 5 min at 10,000 *g*. A single sample contained ~100 A_{600} units of cells. Measurements were routinely carried out in triplicate. The samples were transferred into microcentrifuge tubes of known weight and centrifuged at RT for 10 min at 15,000 *g*. The supernatants were carefully removed, and the sample was measured gravimetrically on an analytical balance. Each sample was dried in a Speed Vac (Savant) vacuum refrigerator for 3 h, and the dry weight of the samples was measured. One molar HCl (0.6 ml) was added to the dry samples and vortexed. The samples were extracted on a rocker table for 24 h and then centrifuged at 15,000 *g* for 5 min. Ca^{2+} measurements were carried out on the supernatants.

$^{45}Ca^{2+}$ uptake was measured as described previously (28). Cells were harvested from a culture in exponential growth (cell density <0.8 A_{600} unit/ml), washed three times in distilled water, and resuspended at a density of 1 A_{600} unit/ml in 40 mM MES-TRIS buffer, pH 5.5, and 20 mM D-Gal or D-Glc. The Ca^{2+} uptake experiment was started with the addition of 1 μCi/ml $^{45}Ca^{2+}$. At the indicated times, 1-ml aliquots were filtered through 0.45-μm Millipore filters prewashed with a solution containing 10 mM $LaCl_3$ and 20 mM $MgCl_2$. Samples were then washed with 5 ml of wash solution before the membranes were collected for scintillation counting. Nonspecific $^{45}Ca^{2+}$ binding at the zero time point was subtracted for each sample.

After the isolation of vacuole-rich membrane fraction, the $^{45}Ca^{2+}$ uptake was measured similarly as described earlier (3). The test medium was slightly different (in mM): 20 MES-TRIS buffer, pH 6.7, 1 ATP, 2 $MgCl_2$, and 2 NaN_3, with 0.5 μCi/ml $^{45}Ca^{2+}$. The incubation was carried out at 30°C for 10 min, and the samples were filtered rapidly through 14,000 molecular weight cutoff membranes with a Millipore filter manifold. The filters were washed twice with ice-cold 20 mM MES-TRIS buffer, pH 6.7, 145 mM KCl, and the membrane-associated counts per minute values were measured.

Ca^{2+} is present in yeast in two kinetically distinguishable pools (9). The $^{45}Ca^{2+}$ exchange was measured as described previously (13). Briefly, wild-type yeast was grown in the absence or presence of 15 mM LiCl in the YP-Gal growth medium for five generations. The medium was supplemented with 5 μCi/ml $^{45}Ca^{2+}$. The cells were harvested, washed, and resuspended in YP-Gal supplemented with 20 mM $CaCl_2$. The cultures were then incubated at 30°C for 40 min, and aliquots of cells were filtered and processed for scintillation counting as described above.

Measurements of cytosolic free Ca^{2+} concentrations. Cytosolic free Ca^{2+} was measured in yeast cells essentially as described previously (5). Briefly, the wild-type strain carrying the pEVP11 plasmid (which carries the apoaequorin gene and the *LEU2* gene as selectable marker) was grown in SM-Glc or SM-Gal medium supplemented with the appropriate amino acids. The cells were then centrifuged and loaded with coelenterazine. For in vivo cytosolic Ca^{2+} measurements, a Berthold 9050 Lumat luminometer was used. Cultures were grown to 0.7–1.0 A_{600} unit/ml. For Gal readdition experiments the cells were preincubated in hexose-free test medium for 2 h. Two A_{600} units of cells were used for a single measurement. After the preincubation period, cells were transferred into sample holders, and the measurement was initiated. After the baseline light emission was measured for ~40 s, 100 mM $CaCl_2$ or 100 mM Gal was injected directly into the sample cuvette. Each experiment was repeated at least three times before results were accepted. Standardization and calculation of results were performed as described previously (28).

Measurement of cellular Glc-1-P and Glc-6-P levels. Wild-type *S. cerevisiae* cells were grown and maintained as described above. For assays of Glc-1-P and Glc-6-P levels, the cells were harvested at a density of 0.8–1 A_{600} unit/ml by centrifugation and resuspended in YP-Gal medium (100 A_{600} units/ml). The cells were preincubated at 30°C for 15 min, and the experiment was initiated by the addition of LiCl. The samples were continuously kept in motion (200 rpm/min) in an environmental shaker incubator. Samples were harvested by pipetting 1 ml of cells into microcentrifuge tubes containing 0.11 ml of 6.67 M perchloric acid. The microcentrifuge tubes also contained ~200 mg of glass beads. After sample addition, the microcentrifuge

tubes were placed on ice for 20 min. Subsequently, samples were vortexed vigorously three times for 1 min and centrifuged at 10,000 *g* for 5 min, and the supernatant was removed. After the neutralization of the supernatant with 5 M KOH (final pH 6.0–6.5), the Glc-6-P and Glc-1-P substrate measurements were carried out according to the method of Bergmayer et al. (6). Because some samples contained Li^+ that can competitively displace Mg^{2+} from PGM, we raised the Mg^{2+} concentration to 5 mM in the test buffer. We found that the highest sample Li^+ concentrations did not significantly affect the results.

Measurement of ATP, ADP, and AMP levels. ATP, ADP, and AMP levels were measured from the same extracts used for Glc-1-P and Glc-6-P determinations. We used a reversed-phase HPLC method slightly modified from that described by Stocchi et al. (41). Briefly, 20 μl of supernatant was mixed with 80 μl of *buffer A* (0.1 M KH_2PO_4, pH 6.0) and filtered through a 0.2-μm syringe filter. Samples were loaded on a Beckman Ultrasphere ODS C18 reversed-phase column (pore size 5 μm, length 250 mm, diameter 4.6 mm). Elution was performed under the following conditions: 9 min at 100% *buffer A*, 6 min at up to 100% *buffer B* [0.1 M KH_2PO_4 containing 10% (vol/vol) HPLC-grade methanol, pH 6.0], and hold for 5 min. The gradient was then returned to *buffer A* in 2 min, and the initial conditions were restored for 5 min. The flow rate was 1.3 ml/min, and detection was performed at 254 nm. Peaks identified were confirmed by coelution with standards. Data were calculated from the peak areas and expressed as "energy charge," using the following formula: energy charge = (ATP + ½ADP)/(ATP + ADP + AMP).

RESULTS

Lithium elevates Ca_t in yeast cells grown in media containing Gal as carbon source. We previously demonstrated (15) that a *S. cerevisiae* mutant lacking the major PGM isoform (*pgm2*Δ) accumulates six to ninefold more Ca_t than a wild-type strain when grown in medium containing Gal, but not Glc, as sole carbon source. Others demonstrated that the presence of Li^+ inhibits PGM activity in wild-type *S. cerevisiae* (26). To determine the effect of Li^+ on cellular Ca^{2+} homeostasis, a wild-type yeast strain and a mutant strain lacking the minor PGM isoform (*pgm1*Δ) were grown in YP media containing Gal or Glc as carbon source. Cultures were also supplemented with 0–15 mM LiCl. Figure 2 shows that the presence of Li^+ in the growth medium caused an elevated Ca_t level in wild-type yeast when Gal was utilized as carbon source (Fig. 2*A*). The maximum level of Ca_t was 4.1-fold higher than that in control (untreated) cells. Also similarly to the *pgm2*Δ mutant, Li^+ slowed the growth rate of the cells in a concentration-dependent manner. In contrast, the presence of Li^+ in the growth medium did not lead to a significant increase in Ca_t in cells grown with Glc as carbon source (Fig. 2*B*). To exclude the possibility that Ca^{2+} influx may occur as a general response to salt stress, we repeated the above experiments with 150 mM NaCl in the medium. No increase in Ca_t was observed under these conditions (Fig. 2).

A strain lacking the minor PGM isoform (*pgm1*Δ) was previously shown to exhibit a modest (10–15%) decrease in PGM activity that did not cause any growth defects in Gal-containing media (14, 15). Similarly, we found that Ca_t levels were comparable when the wild-type and *pgm1*Δ strains were grown under these conditions. However, the *pgm1*Δ strain accumulated significantly more Ca^{2+} when this growth medium was supplemented with Li^+ (Fig. 2*A*). The maximum level of Ca_t was 6.3-fold higher than the values measured when this strain was grown in the absence of Li^+. As before, the addition of Li^+ had no effect on Ca_t when the *pgm1*Δ strain

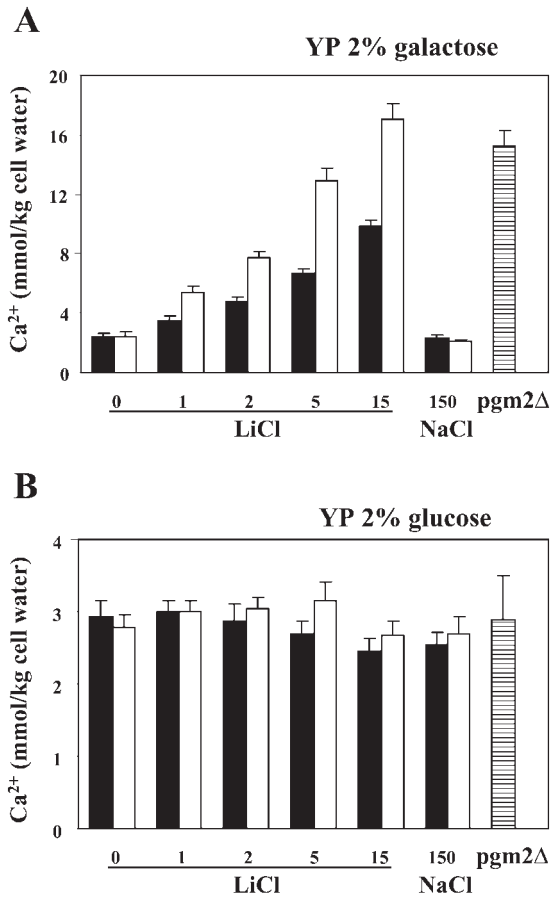

Fig. 2. Total cellular Ca^{2+} levels in wild-type (solid bars) and *pgm1*Δ mutant (open bars) strains of *Saccharomyces cerevisiae*. Cells were grown in yeast extract-peptone (YP) medium containing 2% D-Gal (*A*) or 2% D-Glc (*B*) in the presence of 0–15 mM LiCl for 5 or 6 generations and harvested in the exponential growth phase for total Ca^{2+} determination. Error bars represent SD; $n = 6$. Striped bars show respective salt stress controls in which cells were incubated in the presence of 150 mM NaCl as well as total Ca^{2+} levels in *pgm2*Δ strains.

was grown with Glc as carbon source (Fig. 2*B*). We also attempted to determine the effect of Li^+ treatment on the *pgm2*Δ mutant strain. We found that even the lowest (1 mM) Li^+ level causes near-complete growth inhibition in Gal-containing media. This observation is not surprising because only ~10% of the wild-type PGM activity remains in the *pgm2*Δ mutant, and it suggests that Li^+ inhibition of this remaining PGM activity cannot be tolerated. Together, these results suggest that the metabolic bottleneck in the conversion of Glc-1-P to Glc-6-P caused by Li^+ inhibition of PGM activity results in a large increase in Ca_t. Not surprisingly, in strains that hold a reduced level of PGM activity (such as the *pgm1*Δ mutant) this Ca^{2+} accumulation is further enhanced.

Li^+ increases the rate of Ca^{2+} uptake in yeast cells but does not alter its intracellular distribution. Our observation that Li^+ elevated Ca_t in cells grown with Gal as carbon source (Fig. 2*A*) suggested that increased Ca^{2+} uptake through the plasma membrane occurs in Li^+-treated cells grown under these conditions. To test this hypothesis, wild-type *S. cerevisiae* cells were grown in media containing Gal as carbon source in the absence or presence of 1 mM LiCl. Cells were then harvested, washed, and resuspended in a Ca^{2+}-uptake buffer with or

without 1 mM LiCl. We found that the uptake of $^{45}Ca^{2+}$ was accelerated roughly twofold when 1 mM LiCl was present in both the growth medium and the uptake buffer (Fig. 3*A*). A similar increase in $^{45}Ca^{2+}$ uptake was observed when cells were grown in Li^+-free medium as long as the Ca^{2+}-uptake buffer contained 1 mM LiCl. This demonstrates that only a 1-min exposure to Li^+ was sufficient to mediate this increase in Ca^{2+} uptake. In contrast, cells grown with Glc as the carbon source did not show any significant Li^+-dependent alterations in $^{45}Ca^{2+}$ uptake (data not shown). These results indicate that Li^+ exposure leads to an increase in Ca^{2+} uptake by a rapid mechanism that does not require de novo protein synthesis.

Intracellular Ca^{2+} in yeast exists in two kinetically distinguishable pools (9). More than 95% of the Ca_t is compartmentalized in the vacuole in a relatively stable polyphosphate-bound form (the "nonexchangeable" or slowly exchangeable pool). The exchangeable pool represents the cytosol-, ER-, and Golgi-localized form of this divalent cation, as well as a small fraction of the huge vacuolar Ca^{2+} pool. We showed previously (15) that the distribution of Ca^{2+} between these two kinetically distinguishable pools was not significantly altered in a *pgm2*Δ mutant. Here, we found no significant difference between the relative size of the exchangeable Ca^{2+} pools in wild-type yeast grown in the presence or absence of 15 mM LiCl (Fig. 3*B*). These results indicate that the Li^+-treated cells grown with Gal as carbon source continued to distribute cellular Ca^{2+} normally between these kinetically distinguishable pools.

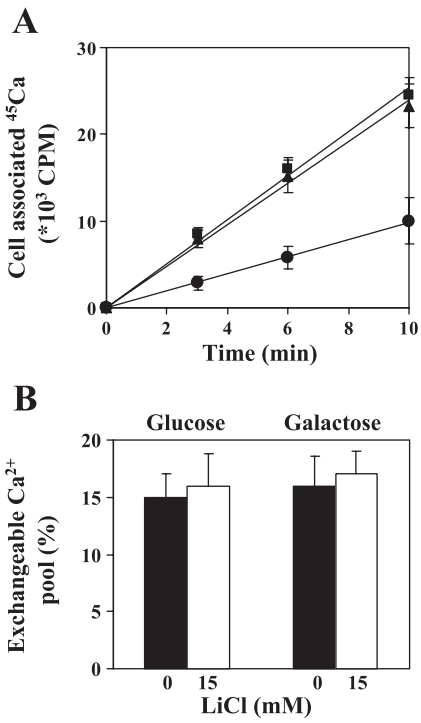

Fig. 3. *A*: $^{45}Ca^{2+}$ uptake in wild-type *S. cerevisiae* cells grown in media containing 2% Gal as carbon source. Control cells were grown in the absence of Li^+ (●). A second culture was grown in medium containing 1 mM LiCl (■), and LiCl was also present when $^{45}Ca^{2+}$ uptake was measured. A third culture was grown in medium without LiCl, but 1 mM LiCl was added to the test medium immediately before $^{45}Ca^{2+}$ was added to the uptake medium (▲). SD are shown; $n = 3$. cpm, Counts per minute. *B*: wild-type yeast was grown in the absence (0) or presence of 15 mM LiCl in YP-Gal growth medium for 5 generations. The medium was supplemented with $^{45}Ca^{2+}$. The cells were harvested, washed, and resuspended in YP-Gal supplemented with 20 mM $CaCl_2$. The cultures were then incubated at 30°C for 40 min. Aliquots of cells were filtered before and after the incubation and processed for scintillation counting. SD are shown; $n = 3$.

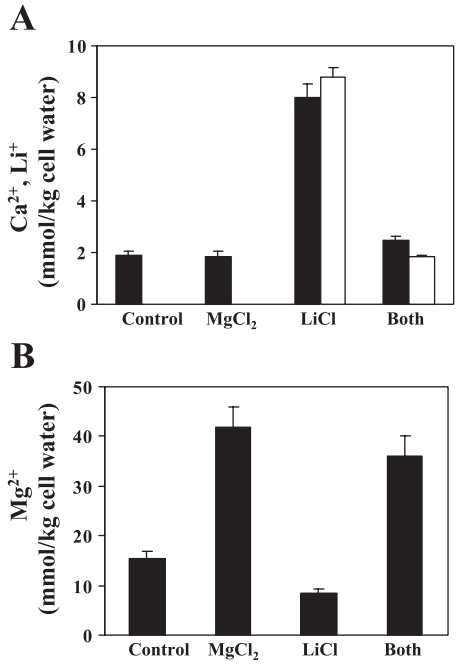

Fig. 4. Total cellular Ca^{2+} (solid bars) and Li^+ (open bars) (*A*) and Mg^{2+} (*B*) levels in wild-type *S. cerevisiae* grown in media containing Gal as carbon source. Except for the control cells, the medium was supplemented with 100 mM $MgCl_2$, 15 mM LiCl, or both (as indicated). SD are shown; $n = 6$.

Magnesium reduces Li^+-induced accumulation of Ca^{2+} in S. cerevisiae. Li^+ inhibits PGM activity by displacing essential Mg^{2+} (35, 36). In addition, Masuda et al. (26) found that Mg^{2+} addition can reverse the Li^+-mediated inhibition of PGM activity in cell homogenates and protect against the toxic effects of Li^+ exposure on yeast cell growth. In light of these findings, we next investigated the effect of Mg^{2+} on Li^+-induced Ca^{2+} accumulation. Figure 4*A* shows that the addition of 100 mM $MgCl_2$ to the growth medium had no significant effect on the Ca_t in wild-type yeast cells grown in medium containing Gal as carbon source. The addition of 15 mM LiCl to the medium resulted in a fourfold increase in Ca_t, whereas the addition of Mg^{2+} largely reversed the Li^+-induced Ca^{2+} accumulation. These results demonstrate that although the addition of Mg^{2+} does not significantly affect Ca_t in control cells, it alleviates the high-Ca_t phenotype found in Li^+-treated cells grown with Gal as carbon source.

Furthermore, a 4.7-fold reduction in the cellular Li^+ level was observed in LiCl + $MgCl_2$-treated cells compared with cells treated with LiCl alone (Fig. 4*A*). We also found that the addition of 100 mM $MgCl_2$ caused a 2.7-fold increase in the cellular Mg^{2+} level (Fig. 4*B*), whereas growth in the presence of 15 mM LiCl reduced the cellular Mg^{2+} concentration 1.8-fold below the level observed in the wild-type control. The cellular Mg^{2+} level remained at 2.3-fold higher than control when both 100 mM $MgCl_2$ and 15 mM LiCl were present in the medium instead of 100 mM $MgCl_2$ alone. The slightly decreased Mg^{2+} level observed when both Li^+ and Mg^{2+} were added together is likely due to competition for entry into the

cell. Accordingly, we found that both the elevation of intracellular Mg^{2+} (4.2-fold) and the reduction of intracellular Li^+ (4.7-fold) contribute to the high intracellular Mg^{2+}-to-Li^+ ratio (17.8) found in LiCl + $MgCl_2$-treated cells over LiCl-treated cells (Mg^{2+}-to-Li^+ ratio = 0.97).

Out of these data two conclusions may be drawn. First, as predicted, extracellular Mg^{2+} prevents the Li^+-induced elevation of Ca_t. Second, unlike in cell lysates, the addition of Mg^{2+} to the medium not only elevates the intracellular Mg^{2+} concentration but also reduces Li^+. Consequently, two accommodating effects result in a very high intracellular Mg^{2+}-to-Li^+ ratio and decrease PGM inhibition within the cell.

Li^+ reverses cellular Glc-1-P-to-Glc-6-P ratio without altering cellular energy charge. It has been shown that either the deletion of the *PGM2* gene or Li^+ inhibition of PGM activity elevates the cellular Glc-1-P level in media containing Gal as carbon source (2, 15, 26). To further address whether a direct link exists between Glc-1-P accumulation and increased Ca^{2+} uptake, we next asked whether the metabolic consequences of Li^+ inhibition of PGM developed within a comparable time period.

Wild-type and *pgm2*Δ yeast strains were grown at 30°C in medium containing Gal as carbon source. An aliquot of the wild-type cells was harvested, and the remainder was immediately resuspended in fresh growth medium containing 15 mM LiCl. Additional aliquots were harvested from the Li^+-treated culture 30 s and 5 min later, and each aliquot was then processed to determine cellular Glc phosphate levels. Figure 5 shows the Glc-6-P and Glc-1-P levels and Glc-1-P-to-Glc-6-P ratios measured in control cells (harvested before the addition of Li^+) and in cells harvested after 30 s or 5 min of Li^+ treatment, respectively. The Glc-1-P-to-Glc-6-P ratio more than doubled in these cells within 30 s of addition of 15 mM LiCl (from 0.33 to 0.79). By the 5-min time point, the Glc-1-P-to-Glc-6-P ratio had increased more than fivefold (from 0.33 to 1.71). Longer incubation times resulted in additional modest increases in the Glc-1-P-to-Glc-6-P ratio in wild-type cells (data not shown). Although this reversal of the Glc-1-P-to-Glc-6-P ratio is due primarily to a large increase in the Glc-1-P concentration, a small decrease in the level of Glc-6-P also occurred. These results demonstrate that the Li^+ inhibition of PGM activity leads to a significant increase in the cellular Glc-1-P-to-Glc-6-P ratio within 30 s of exposure, with a further

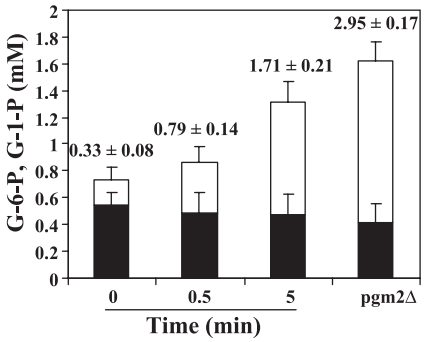

Fig. 5. Glc-6-P (solid bars) and Glc-1-P (open bars) levels and Glc-1-P-to-Glc-6-P ratios (values over bars) in wild-type *S. cerevisiae* grown in medium containing Gal as carbon source and then resuspended in fresh medium supplemented with 15 mM LiCl. Samples were taken at 0, 0.5, and 5 min. SD are shown; $n = 4$.

increase occurring on longer incubation. In addition, the rapid changes in the Glc-1-P-to-Glc-6-P ratio occur within a short time frame similar to that of the increase in $^{45}Ca^{2+}$ uptake (see Fig. 3), suggesting that these two responses are related. We also note that the Glc-1-P-to-Glc-6-P ratio is significantly lower in Li^+-treated wild-type cells compared with the *pgm2*Δ mutant. This indicates that a more severe metabolic bottleneck occurs when the strain is completely unable to express the major isoform of this enzyme.

A variety of physiological conditions that alter steady-state cellular ATP levels or, more importantly, the cellular energy charge [(ATP + ½ADP)/(ATP + ADP + AMP)] could result in significant alterations in the relative balance of various intracellular ions. Consequently, energy-depleted cells tend to contain more Na^+ and Ca^{2+} and less K^+ and Mg^{2+}. To determine whether this could be responsible for the observed changes in intracellular Ca^{2+} levels, we next asked whether Li^+ treatment causes an alteration in the cellular energy charge. Wild-type yeast cells were again grown with either Glc or Gal as carbon source, and 15 mM LiCl was added to the cultures two generations (3 h) before harvesting. The cells were then processed for the determination of ATP, ADP, and AMP levels. We found that the energy charge of Li^+-treated cells was not significantly different from those incubated without Li^+ when grown with either Glc (0.618 in untreated vs. 0.609 in Li^+ treated), or Gal (0.682 in untreated vs. 0.678 in Li^+ treated) as carbon source. These results indicate that the changes in the cellular Ca^{2+} level following Li^+ treatment were not due to a perturbation of the energy charge.

Li^+ reduces transient elevation of cytosolic Ca^{2+} response in S. cerevisiae. Yeast cells respond to a variety of stimuli, such as exposure to mating pheromones or changes in carbon source, osmolarity, and ionic composition of the environment, with a transient elevation of the cytosolic Ca^{2+} (TECC) response (5, 19, 21, 32, 42). As described above, we observed an accelerated rate of $^{45}Ca^{2+}$ uptake when yeast cells were exposed to Li^+ (Fig. 3). We also previously reported (15) that a similar increase in Ca^{2+} uptake was associated with a *pgm2*Δ mutant and showed that the TECC response induced by Gal readdition to yeast cells starved for a carbon source is reduced in the *pgm2*Δ strain.

To determine whether exposure to Li^+ also alters the TECC response, we preincubated cells in a medium lacking a carbon source in the presence or absence of 10 mM LiCl and then measured free cytosolic Ca^{2+} levels in response to the addition of 100 mM Gal. The basal cytosolic Ca^{2+} level under both conditions before Gal addition was roughly 65 nM (although the basal level in Li^+-treated cells was slightly lower than that in untreated cells). We found that the normal TECC response stimulated by the addition of Gal resulted in a peak cytosolic Ca^{2+} concentration of 200 nM (Fig. 6*A*). In contrast, the TECC response induced in Li^+-treated cells in the same manner resulted in a peak cytosolic Ca^{2+} concentration of only 130 nM. The recovery phase following the TECC response was similar in both Li^+-treated and control cells.

Normal yeast SM medium contains 1 mM $CaCl_2$. However, wild-type yeast strains can grow normally in the presence of 100 mM $CaCl_2$. Previous studies have shown that the abrupt exposure of yeast cells to this high level of $CaCl_2$ results in a TECC response that differs from that induced by hexose addition to cells starved of a carbon source (42). Under these

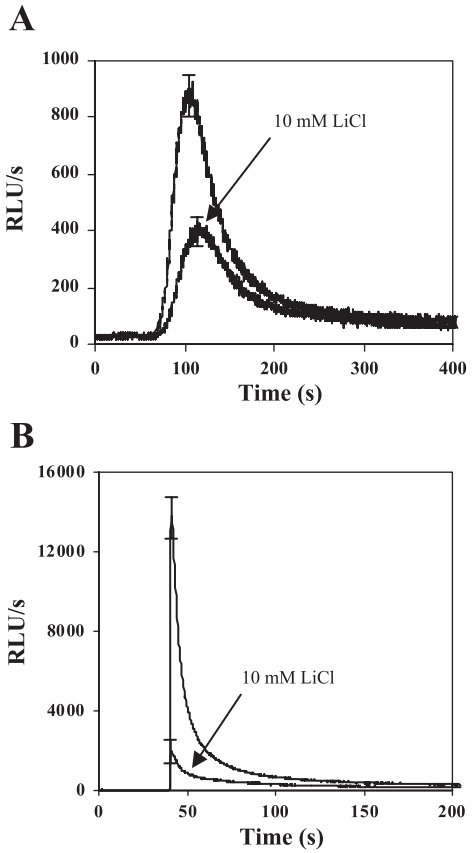

Fig. 6. *A*: transient elevation of cytosolic Ca^{2+} (TECC) response induced by the injection of 100 mM Gal. Before the injection, wild-type *S. cerevisiae* cells were grown in medium containing Gal as carbon source and then incubated in hexose-free test medium for 2 h in the absence or presence of 10 mM LiCl. Intracellular Ca^{2+} measurements were carried out in *S. cerevisiae* cells expressing apoaequorin as described in MATERIALS AND METHODS. SD are shown at the highest peak levels; $n = 4$. *B*: TECC response induced by the injection of 100 mM $CaCl_2$. Wild-type *S. cerevisiae* cells were grown in medium containing Gal as carbon source. Before the injection, cells were incubated in test medium for 20 min in the absence or presence of 10 mM LiCl. SD shown at the highest peak levels; $n = 4$. RLU, Relative Luminescence Unit.

conditions, the sudden elevation of extracellular Ca^{2+} results in an immediate Ca^{2+} surge into the cytosol that results in a sharp TECC response followed by a rapid reduction in the level of free cytosolic Ca^{2+} as plasma membrane Ca^{2+} channels close and organellar Ca^{2+} transporters are activated to increase sequestration into intracellular compartments. Figure 6*B* shows how *S. cerevisiae* cells grown with Gal as carbon source respond to the injection of 100 mM $CaCl_2$ into the incubation medium. As before, the basal cytosolic Ca^{2+} level under both conditions was roughly 65 nM. We found that the TECC response following the addition of 100 mM $CaCl_2$ to untreated cells resulted in a peak cytosolic concentration of ~1,010 nM. In contrast, the response observed in Li^+-treated cells was reduced to a peak level of only 310 nM. Thus the TECC response was again significantly reduced in Li^+-treated cells. These data indicate that Li^+ exposure results in a reduction in the magnitude of the TECC response to various stimuli. Because we had previously shown that Li^+ treatment increases the basal rate of cellular Ca^{2+} uptake, this decrease in the magnitude of the TECC response suggests that Li^+ activates organellar Ca^{2+} sequestration. Therefore, despite the increased Ca^{2+} uptake, the TECC response observed is smaller than normal.

Increased Ca_t level in Li^+-treated cells is caused by excessive vacuolar Ca^{2+} uptake. Intracellular Ca^{2+} storage occurs primarily in two organelles in *S. cerevisiae*. Previous studies showed that >90% of the Ca_t is located in the vacuole, where the Ca^{2+}-ATPase Pmc1p and the Ca^{2+}/H^+ antiporter Vcx1p facilitate Ca^{2+} uptake and accumulation (10, 20, 34). In addition, the Golgi-located Ca^{2+}-ATPase Pmr1p assists in intracellular Ca^{2+} compartmentalization under certain conditions (12, 33, 39). Previous studies showed that a *vcx1*Δ*/pmc1*Δ mutant that is defective for vacuolar Ca^{2+} uptake exhibits a reduced Ca_t level and decreased Ca^{2+} tolerance (28, 29), whereas a *pmr1*Δ mutant that is impaired in Golgi Ca^{2+} uptake has an increased rate of cellular Ca^{2+} uptake (20).

To determine whether an elevated rate of vacuolar Ca^{2+} sequestration is responsible for the observed effects of Li^+ on cellular Ca^{2+} homeostasis, wild-type, *vcx1*Δ, *pmc1*Δ, and *vcx1*Δ*/pmc1*Δ strains of *S. cerevisiae* were grown in YP-Gal medium in the presence or absence of 15 mM LiCl. Both the wild-type and *vcx1*Δ strains exhibited a similar fourfold increase in Ca_t when 15 mM Li^+ was present in the medium (Fig. 7*A*). The *pmc1*Δ mutant showed a smaller increase (1.8-fold) under these conditions, whereas the *vcx1*Δ*/pmc1*Δ strain grown in the presence of LiCl exhibited a level of Ca_t that was only 1.2-fold higher than the untreated control. We also found that a *pmr1*Δ strain exhibited an increase in Ca_t in response to Li^+ treatment that was similar to the wild-type strain (data not shown). These data suggest that the primary consequence of Li^+ exposure is an increased level of vacuolar Ca^{2+} accumulation and the increased rate of Ca^{2+} uptake across the plasma membrane is a secondary consequence of

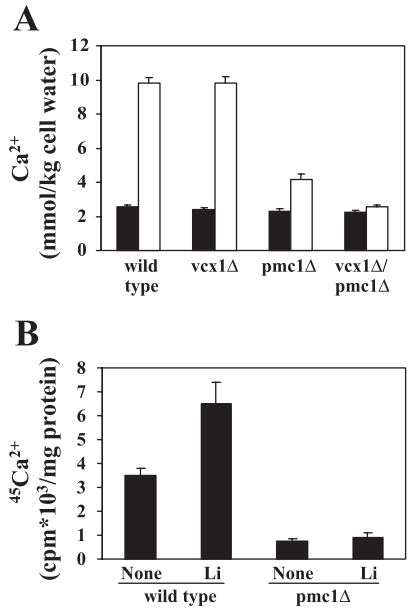

Fig. 7. *A*: total cellular Ca^{2+} levels in wild-type, *vcx1*Δ, *pmc1*Δ, and *vcx1*Δ*/pmc1*Δ *S. cerevisiae* strains grown in media containing Gal as carbon source in the absence (solid bars) or presence (open bars) of 15 mM LiCl. SD are shown; $n = 6$. *B*: $^{45}Ca^{2+}$ uptake into membrane vesicles of wild-type and *pmc1*Δ strains. Isolated vacuolar membrane vesicles were incubated in the absence (None) or presence of 1 mM LiCl and $^{45}Ca^{2+}$-containing test medium. SD are shown; $n = 3$.

excessive vacuolar uptake. Of the two known vacuolar Ca^{2+} transport mechanisms, Ca^{2+} transport by Pmc1p appears to be more important for this response than the Ca^{2+}/H^{+} exchanger Vcx1p. However, Vcx1p appears to be capable of contributing to a small increase in vacuolar Ca^{2+} transport in the *pmc1*Δ mutant, because the *vcx1*Δ*/pmc1*Δ double mutant showed a lower Ca_t level than the *pmc1*Δ strain after Li^{+} exposure. This conclusion is consistent with the results of previous studies that described partially overlapping roles for these Ca^{2+} transporters (28, 29).

Isolated and partially purified vacuolar vesicles were also used to examine the effect of Li^{+} on $^{45}Ca^{2+}$ uptake into this organelle (Fig. 7*B*). Wild-type and *pmc1*Δ strains were grown in YP-Gal media in the absence or presence of 1 mM LiCl, and a vacuole-enriched membrane fraction was prepared as previously described (3, 39). $^{45}Ca^{2+}$ uptake measurements were carried out in test buffer in the absence or presence of 1 mM LiCl, respectively. We observed a 1.9-fold increase in $^{45}Ca^{2+}$ uptake in vesicles isolated from wild-type cells cultured in the presence of Li^{+}, but a much smaller 1.2-fold increase was induced in the *pmc1*Δ mutant by the same treatment. These results further support the role of *PMC1* in Li^{+}-induced Ca^{2+} accumulation.

The low level of PGM activity caused by the deletion of the *PGM2* gene results in a slow-growth phenotype when a *pgm2*Δ strain is grown in medium containing Gal as carbon source (15). This slow-growth phenotype is related to the elevated Ca^{2+} accumulation that occurs in this strain, and this phenotype is partially suppressed in a *pgm2*Δ*/pfk2*Δ double mutant, in which a more normal Glc-1-P-to-Glc-6-P ratio is restored and Ca_t is reduced (2). We next asked whether the *pfk2*Δ mutation can also reverse the elevated Ca_t caused by Li^{+} treatment. We found that the *pfk2*Δ mutation effectively suppressed the high-Ca_t phenotype of the Li^{+}-treated cells (Fig. 8). A significant increase in Ca_t was not observed in the *pfk2*Δ strain in the 0–5 mM Li^{+} range, and at 15 mM Li^{+} a Ca_t increase of only 1.7-fold was observed. The level of Ca^{2+} accumulation in the *pfk2*Δ strain grown in the presence of 15 mM Li^{+} was <50% of the level observed in the wild-type strain grown under the same conditions.

It has also been shown that Li^{+} reduces the growth rate of the wild-type strain to a level that is similar to the growth rate observed in a *pgm2*Δ strain grown in medium containing Gal as carbon source (26). Because the results described above indicated that the *pmc1*Δ mutation suppresses the high-Ca_t phenotype, this suggested that the *pmc1*Δ mutant might also grow better in media containing LiCl than the wild-type strain. This prediction was found to be correct, as the *pmc1*Δ strain was found to grow faster on YP-Gal plates supplemented with 15 mM LiCl than either the wild-type or *vcx1*Δ strain (Fig. 9). Consistent with the observation that the *vcx1*Δ*/pmc1*Δ strain largely reverses the high-Ca^{2+} phenotype (Fig. 7*A*), we found that the *vcx1*Δ*/pmc1*Δ strain grew significantly faster than a strain carrying the *pmc1*Δ mutation alone. Finally, we also observed an intermediate level of suppression of the Li^{+}-mediated growth inhibition in a *pfk2*Δ strain (data not shown). Together these results suggest that Li^{+} exerts its effects primarily by enhancing Ca^{2+} transport into the vacuole. Because the targeted deletion of the *PMC1* gene partially suppresses not only the high-Ca_t but also the slow-growth phenotype of

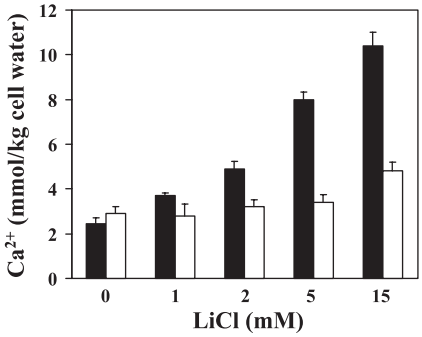

Fig. 8. Total cellular Ca^{2+} levels in wild-type (solid bars) and *pfk2*Δ mutant (open bars) strains of *S. cerevisiae*. Cells were grown in YP medium containing 2% D-Gal in the presence of 0–15 mM LiCl for 5 or 6 generations and harvested in the exponential growth phase for total Ca^{2+} determination. SD are shown; $n = 3$.

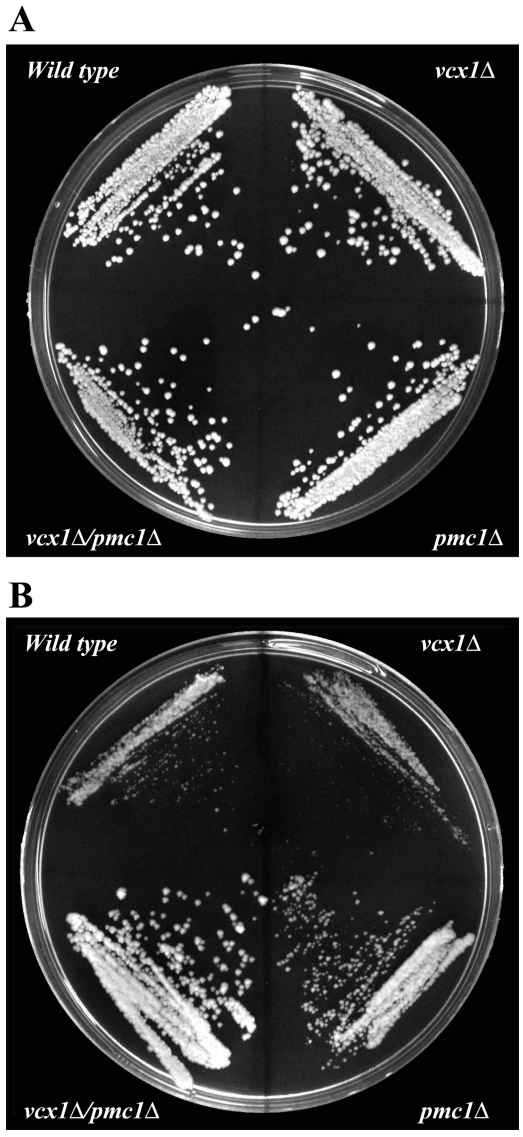

Fig. 9. Disruption of the *PMC1* gene suppresses Li^{+}-induced, galactose-specific growth defects. Wild-type and *vcx1*Δ, *pmc1*Δ, and *vcx1*Δ*/pmc1*Δ strains were grown on YP-Gal plates (*A*) and YP-Gal plates supplemented with 15 mM LiCl (*B*).

Li^+-treated cells, it appears that the vacuolar Ca^{2+}-ATPase Pmc1p plays a pivotal role in this process.

DISCUSSION

Li^+ has been shown to compete with Mg^{2+} for a functionally important binding site in mammalian PGM because of similarities in their hydrated radii (35, 36). The resulting Li^+-PGM complex is almost completely devoid of enzymatic activity. Recently, Masuda et al. (26) reported that Li^+ mediates an inhibition of PGM activity in the yeast *S. cerevisiae*. We previously showed (15) that reduced PGM activity results in elevated Ca_t in a *pgm2*Δ mutant grown in media containing Gal as the carbon source.

In the present study we found that Li^+ elevates Ca_t 4.1-fold in wild-type *S. cerevisiae* grown in media containing Gal as carbon source and 6.3-fold in a mutant strain (*pgm1*Δ) that has a modest (10–20%) decrease in PGM protein (Fig. 2*A*). Consequently, Ca_t appears to relate inversely to PGM activity in cells grown with Gal as the carbon source. In contrast, the Ca_t level remained unaltered when these cells were grown in the presence of identical Li^+ concentrations in media containing Glc as carbon source (Fig. 2*B*), where the PGM enzyme levels are much lower because cells do not depend on the activity of this enzyme for the entry of metabolites into the glycolytic pathway (Fig. 1; Ref. 14). The carbon source dependence of this effect is consistent with the previous conclusion that alterations in Ca^{2+} homeostasis caused by changes in PGM activity are determined by the metabolic flow through the reversible PGM enzymatic reaction (and the resulting relative levels of Glc-1-P and Glc-6-P) (2, 15).

We also demonstrated that the uptake of Ca^{2+} into Li^+-treated cells is significantly accelerated over the Ca^{2+} uptake measured in control cells (Fig. 3*A*). Remarkably, this increase was found to begin within 1 min of Li^+ exposure. Because the cellular Glc-1-P-to-Glc-6-P ratio more than doubles within 30 s of Li^+ addition (Fig. 5), we propose that the rapid increase of Glc-1-P, and the resulting high Glc-1-P-to-Glc-6-P ratio, is the most likely inducer of this response. These observations also suggest that the effect on Ca^{2+} homeostasis is not due to the induction of de novo gene expression and is probably due to a signaling mechanism.

We previously observed (15) a similar correlation between the cellular Glc-1-P-to-Glc-6-P ratio and Ca_t in a *S. cerevisiae* *pgm2*Δ mutant that lacks the major isoform of PGM. It was also shown that the disruption of a second gene (*pfk*Δ) encoding the β-subunit of phosphofructokinase in a *pgm2*Δ strain results in dual metabolic blocks that elevated the levels of both Glc-1-P and Glc-6-P (2). Remarkably, the Ca^{2+}-related phenotypes of the *pgm2*Δ strain were largely eliminated in the *pgm2*Δ*/pfk2*Δ double mutant. Therefore, one might assume that the effect of Li^+ on Ca_t should also be abrogated in a *pfk2*Δ mutant, which would similarly correct the cellular Glc-1-P-to-Glc-6-P ratio. Indeed, we found that the *pfk2*Δ strain had significantly lower Ca_t levels than the wild-type strain when grown in Gal media supplemented with LiCl (Fig. 8).

The hypothesis that Li^+ mimics the Ca^{2+} homeostasis-related phenotype of the *pgm2*Δ strain through its ability to inhibit PGM activity is further strengthened by the observation that Mg^{2+} reverts the Li^+-induced elevation of Ca_t (Fig. 4). Unlike cell homogenates in which competition for the functionally important Mg^{2+} binding site of PGM would correspond to the actual Mg^{2+} and Li^+ levels added, the addition of extracellular Mg^{2+} both elevates the intracellular Mg^{2+} levels and decreases the intracellular Li^+ concentration. Importantly, extracellular Mg^{2+} alone had little if any effect on Ca_t, indicating that it affects Ca_t in Li^+-treated cells by decreasing the inhibition of PGM activity.

A transient elevation of cytosolic Ca^{2+} occurs in *S. cerevisiae* immediately after the addition of mating pheromone, Ca^{2+}, or hexoses or an abrupt change in the osmolarity of the environment (5, 32, 42). In the present work, we found that the basal cytosolic Ca^{2+} levels were slightly lower in Li^+-treated cells relative to untreated control cells. The TECC responses caused by $CaCl_2$ shock (sudden Ca^{2+} overflow) or the addition of Gal to cells starved of a carbon source (Glc phosphate-induced Ca^{2+} uptake through the plasma membrane) were significantly reduced when Li^+ was present in the culture medium (Fig. 6). These results indicate that Li^+ alters a common component involved in the propagation of various TECC responses. Because Ca^{2+} uptake across the plasma membrane increases almost immediately on Li^+ exposure, a reduced rate of Ca^{2+} uptake cannot account for the diminished TECC response. Instead, we propose that the observed reduction in the TECC response results from an increased rate of Ca^{2+} removal from the cytosol into an intracellular compartment. Consistent with this hypothesis is the finding that the excessive Ca^{2+} accumulation and slow-growth phenotype induced by Li^+ treatment could be reduced by disruption of the gene encoding the vacuolar Ca^{2+}-ATPase Pmc1p (Figs. 7 and 9). These results are also consistent with our recent observation (3) that the disruption of the *PMC1* gene partially suppresses the Ca^{2+}-related phenotype of the *pgm2*Δ mutant. The results of the current work also suggest that deletion of the genes encoding both the vacuolar Ca^{2+}/H^+ antiporter Vcx1p and the Ca^{2+}-ATPase Pmc1p causes a more complete suppression of the Li^+-mediated Ca^{2+} phenotype than disruption of the *PMC1* gene alone. This observation is consistent with an earlier report that the two structurally and functionally distinct vacuolar Ca^{2+} transporters play partially overlapping roles. For example, it was shown previously that the Ca^{2+}-sensitive phenotype of the *pmc1*Δ mutant is further exacerbated in the *vcx1*Δ*/pmc1*Δ double mutant (15).

These results, and our earlier observation that the Glc-1-P-to-Glc-6-P ratio is important for proper Ca^{2+} homeostasis, lead us to propose the following sequence of events. First, Li^+ inhibits PGM activity and alters the cellular Glc-1-P-to-Glc-6-P ratio. Second, the altered Glc phosphate levels stimulate vacuolar Ca^{2+} uptake by the Ca^{2+}-ATPase Pmc1p by a currently unknown mechanism. Third, the increased rate of vacuolar Ca^{2+} uptake reduces basal cytosolic (and subsequently ER) Ca^{2+} levels, leading to an induction of the unfolded protein response within the ER lumen (3). Finally, plasma membrane Ca^{2+} channels open to increase Ca^{2+} uptake in an attempt to restore the normal resting steady-state cytosolic Ca^{2+} level.

As yet, we do not understand how Glc phosphates regulate vacuolar Ca^{2+} uptake through the action of PMC1. In a previous study, it was shown that Glc phosphates were unable to activate $^{45}Ca^{2+}$ uptake directly into vesicles derived from vacuolar membranes (3). It has also been shown that the inhibition of calcineurin with cyclosporin A prevents growth of

the *pgm2*Δ strain, suggesting that some downstream consequence of calcineurin activity is essential for the viability of this strain (15). However, we measured only a modest increase in *PMC1* mRNA abundance in the *pgm2*Δ strain relative to the wild-type strain (unpublished results). Because Ca^{2+} accumulation is triggered within a minute of Li^{+} exposure, de novo protein synthesis is clearly not required for this response. These results lead us to conclude that the calmodulin-calcineurin signaling pathway must be involved in this regulatory circuit. However, the downstream signaling targets that modulate vacuolar Ca^{2+} uptake remain to be identified.

In a recent study, Mulet and coworkers (30) reported that trehalose 6-phosphate synthase (TPS)1 activity alters the ion transport characteristics of the K^{+} channels TRK1 and TRK2 through the modulation of cellular Glc phosphate levels. They also noted that like TPS1, PGM and hexokinase 2 are also capable of altering the levels of Glc phosphates and that elevated Glc phosphate levels activate TRK by way of the calcineurin pathway (30). Furthermore, the involvement of HAL4 and HAL5 protein kinases was also described in that study. In light of the current work and another recent study (3), Glc phosphates are clearly emerging as important regulators of intracellular cation homeostasis.

Despite lithium being the "oldest" drug used in the treatment of bipolar disorder, the complex molecular mechanisms of Li^{+} action remain a scientifically challenging problem. Because yeast and mammalian cells share many common characteristics at the level of basic metabolism, the use of the yeast model system may represent an extremely useful tool in elucidating how Li^{+} specifically influences Ca^{2+} signaling pathways through its effect on PGM. In light of the results of the current study, the relative importance of PGM as a moderator of intracellular signal transduction pathways in mammalian cells should clearly be explored in greater detail. Such studies could provide further insights into the mechanism(s) coupling Glc metabolism to Ca^{2+} homeostasis and should further elucidate whether the ability of Li^{+} to inhibit PGM activity plays a significant role in its therapeutic benefits for patients with bipolar disorders.

ACKNOWLEDGMENTS

We thank Sarolta Bácskai, Ibolya Lamár, and Éva Moravcsik for valuable technical assistance.

GRANTS

This work was supported by Hungarian Scientific Research Fund Grants F-038149 (to P. Csutora), T-038144 (to A. Miseta), T-032043 to (K. Sipos), and American Heart Association Southeast Affiliate Grant 0255121B (to D. M. Bedwell).

REFERENCES

1. **Agranoff BW and Fisher SK.** Inositol, lithium, and the brain. *Psychopharmacol Bull* 35: 5–18, 2001.
2. **Aiello DP, Fu L, Miseta A, and Bedwell DM.** Intracellular glucose 1-phosphate and glucose 6-phosphate levels modulate Ca^{2+} homeostasis in *Saccharomyces cerevisiae*. *J Biol Chem* 277: 45751–45758, 2002.
3. **Aiello DP, Fu L, Miseta A, Sipos K, and Bedwell DM.** The Ca^{2+} defects in a *pgm2*Δ strain of *Saccharomyces cerevisiae* are caused by excessive vacuolar Ca^{2+} uptake mediated by the Ca^{2+}-ATPase Pmc1p. *J Biol Chem* 279: 38495–38502, 2004.
4. **Allison JH and Stewart MA.** Reduced brain inositol in lithium-treated rats. *Nat New Biol* 233: 267–268, 1971.
5. **Batiza AF, Schulz T, and Masson PH.** Yeast respond to hypotonic shock with a calcium pulse. *J Biol Chem* 271: 23357–23362, 1996.
6. **Bergmayer HU, Bergmayer J, and Grasl M.** Enzymatic determination of glucose metabolites. In: *Methods of Enzymatic Analysis* (3rd ed.), edited by Bergmayer HU. Weinheim, Germany: Verlag Chemie, 1984, p. 185–198.
7. **Berridge MJ.** The Albert Lasker Medical Awards. Inositol trisphosphate, calcium, lithium, and cell signaling. *JAMA* 262: 1834–1841, 1989.
8. **Berridge MJ, Downes CP, and Hanley MR.** Lithium amplifies agonist-dependent phosphatidylinositol responses in brain and salivary glands. *Biochem J* 206: 587–595, 1982.
9. **Cunningham KW and Fink GR.** Ca^{2+} transport in *Saccharomyces cerevisiae*. *J Exp Biol* 196: 157–166, 1994.
10. **Cunningham KW and Fink GR.** Calcineurin-dependent growth control in *Saccharomyces cerevisiae* mutants lacking PMC1, a homolog of plasma membrane Ca^{2+} ATPases. *J Cell Biol* 124: 351–363, 1994.
11. **Dinan TG.** Lithium in bipolar mood disorder. *BMJ* 324: 989–990, 2002.
12. **Durr G, Strayle J, Plemper R, Elbs S, Klee SK, Catty P, Wolf DH, and Rudolph HK.** The medial-Golgi ion pump Pmr1 supplies the yeast secretory pathway with Ca^{2+} and Mn^{2+} required for glycosylation, sorting, and endoplasmic reticulum-associated protein degradation. *Mol Biol Cell* 9: 1149–1162, 1998.
13. **Eilam Y, Othman M, and Halachmi D.** Transient increase in Ca^{2+} influx in *Saccharomyces cerevisiae* in response to glucose: effects of intracellular acidification and cAMP levels. *J Gen Microbiol* 136: 2537–2543, 1990.
14. **Fu L, Bounelis P, Dey N, Browne BL, Marchase RB, and Bedwell DM.** The posttranslational modification of phosphoglucomutase is regulated by galactose induction and glucose repression in *Saccharomyces cerevisiae*. *J Bacteriol* 177: 3087–3094, 1995.
15. **Fu L, Miseta A, Hunton D, Marchase RB, and Bedwell DM.** Loss of the major isoform of phosphoglucomutase results in altered calcium homeostasis in *Saccharomyces cerevisiae*. *J Biol Chem* 275: 5431–5440, 2000.
16. **Gould TD, Chen G, and Manji HK.** Mood stabilizer psychopharmacology. *Clin Neurosci Res* 2: 193–212, 2002.
17. **Gould TD and Manji HK.** The Wnt signaling pathway in bipolar disorder. *Neuroscientist* 8: 497–511, 2002.
18. **Gould TD, Quiroz JA, Singh J, Zarate CA, and Manji HK.** Emerging experimental therapeutics for bipolar disorder: insights from the molecular and cellular actions of current mood stabilizers. *Mol Psychiatry* 9: 734–755, 2004.
19. **Halachmi D and Eilam Y.** Cytosolic and vacuolar Ca^{2+} concentrations in yeast cells measured with the Ca^{2+}-sensitive fluorescence dye indo-1. *FEBS Lett* 256: 55–61, 1989.
20. **Halachmi D and Eilam Y.** Elevated cytosolic free Ca^{2+} concentrations and massive Ca^{2+} accumulation within vacuoles, in yeast mutant lacking PMR1, a homolog of Ca^{2+}-ATPase. *FEBS Lett* 392: 194–200, 1996.
21. **Iida H, Yagawa Y, and Anraku Y.** Essential role for induced Ca^{2+} influx followed by $[Ca^{2+}]_i$ rise in maintaining viability of yeast cells late in the mating pheromone response pathway. A study of $[Ca^{2+}]_i$ in single *Saccharomyces cerevisiae* cells with imaging of fura-2. *J Biol Chem* 265: 13391–13399, 1990.
22. **Kellermayer R, Aiello DP, Miseta A, and Bedwell DM.** Extracellular calcium sensing contributes to excess calcium accumulation and vacuolar fragmentation in *S. cerevisiae*. *J Cell Sci* 15: 1637–1646, 2003.
23. **Klein PS and Melton DA.** A molecular mechanism for the effect of lithium on development. *Proc Natl Acad Sci USA* 93: 8455–8459, 1996.
24. **Manji HK, Moore GJ, and Chen G.** Bipolar disorder: leads from the molecular and cellular mechanisms of action of mood stabilizers. *Br J Psychiatry Suppl* 178: s107–s119, 2001.
25. **Marchase RB, Bounelis P, Brumley LM, Dey N, Browne B, Auger D, Fritz TA, Kulesza P, and Bedwell DM.** Phosphoglucomutase in *Saccharomyces cerevisiae* is a cytoplasmic glycoprotein and the acceptor for a Glc-phosphotransferase. *J Biol Chem* 268: 8341–8349, 1993.
26. **Masuda CA, Xavier MA, Mattos KA, Galina A, and Montero-Lomeli M.** Phosphoglucomutase is an in vivo lithium target in yeast. *J Biol Chem* 276: 37794–37801, 2001.
27. **Miseta A, Bogner P, Berenyi E, Kellermayer M, Galambos C, Wheatley DN, and Cameron IL.** Relationship between cellular ATP, potassium, sodium and magnesium concentrations in mammalian and avian erythrocytes. *Biochim Biophys Acta* 1175: 133–139, 1993.
28. **Miseta A, Fu L, Kellermayer R, Buckley J, and Bedwell DM.** The Golgi apparatus plays a significant role in the maintenance of Ca^{2+} homeostasis in the *vps33*Δ vacuolar biogenesis mutant of *Saccharomyces cerevisiae*. *J Biol Chem* 274: 5939–5947, 1999.

29. **Miseta A, Kellermayer R, Aiello DP, Fu L, and Bedwell DM.** The vacuolar Ca^{2+}/H^{+} exchanger Vcx1p/Hum1p tightly controls cytosolic Ca^{2+} levels in *S. cerevisiae. FEBS Lett* 451: 132–136, 1999.
30. **Mulet JM, Alejandro S, Romero C, and Serrano R.** The trehalose pathway and intracellular glucose phosphates as modulators of potassium transport and general cation homeostasis in yeast. *Yeast* 21: 569–582, 2004.
31. **Muller-Oerlinghausen B, Berghofer A, and Bauer M.** Bipolar disorder. *Lancet* 359: 241–247, 2002.
32. **Nakajima-Shimada J, Iida H, Tsuji FI, and Anraku Y.** Monitoring of intracellular calcium in *Saccharomyces cerevisiae* with an apoaequorin cDNA expression system. *Proc Natl Acad Sci USA* 88: 6878–6882, 1991.
33. **Okorokov LA and Lehle L.** Ca^{2+}-ATPases of *Saccharomyces cerevisiae*: diversity and possible role in protein sorting. *FEMS Microbiol Lett* 162: 83–91, 1998.
34. **Pozos TC, Sekler I, and Cyert MS.** The product of HUM1, a novel yeast gene, is required for vacuolar Ca^{2+}/H^{+} exchange and is related to mammalian Na^{+}/Ca^{2+} exchangers. *Mol Cell Biol* 16: 3730–3741, 1996.
35. **Ray WJ Jr, Post CB, and Puvathingal JM.** Comparison of rate constants for (PO^{3-}) transfer by the Mg(II), Cd(II), and Li(I) forms of phosphoglucomutase. *Biochemistry* 28: 559–569, 1989.
36. **Ray WJ Jr, Szymanki ES, and Ng L.** The binding of lithium and of anionic metabolites to phosphoglucomutase. *Biochim Biophys Acta* 522: 434–442, 1978.
37. **Sassi RB and Soares JC.** Emerging therapeutic targets in bipolar mood disorder. *Expert Opin Ther Targets* 5: 587–599, 2001.
38. **Schou M.** Lithium treatment at 52. *J Affect Disord* 67: 21–32, 2001.
39. **Sorin A, Rosas G, and Rao R.** PMR1, a Ca^{2+}-ATPase in yeast Golgi, has properties distinct from sarco/endoplasmic reticulum and plasma membrane calcium pumps. *J Biol Chem* 272: 9895–9901, 1997.
40. **Stambolic V, Ruel L, and Woodgett JR.** Lithium inhibits glycogen synthase kinase-3 activity and mimics wingless signalling in intact cells. *Curr Biol* 6: 1664–1668, 1996.
41. **Stocchi V, Cucchiarini L, Magnani M, Chiarantini L, Palma P, and Crescentini G.** Simultaneous extraction and reverse-phase high-performance liquid chromatographic determination of adenine and pyridine nucleotides in human red blood cells. *Anal Biochem* 146: 118–124, 1985.
42. **Tokes-Fuzesi M, Bedwell DM, Repa I, Sipos K, Sumegi B, Rab A, and Miseta A.** Hexose phosphorylation and the putative calcium channel component Mid1p are required for the hexose-induced transient elevation of cytosolic calcium response in *Saccharomyces cerevisiae. Mol Microbiol* 44: 1299–1308, 2002.
43. **Williams RS and Harwood AJ.** Lithium therapy and signal transduction. *Trends Pharmacol Sci* 21: 61–64, 2000.
44. **York JD, Ponder JW, and Majerus PW.** Definition of a metal-dependent/Li^{+}-inhibited phosphomonoesterase protein family based upon a conserved three-dimensional core structure. *Proc Natl Acad Sci USA* 92: 5149–5153, 1995.